12. Wolf H, Nacke C, Kaiser K, et al. In vitro uptake von technetium-99m-tetrofosmin, technetium-99m-sestamibi and thallium-201 in Tumorzellkulturen [Abstract]. *Nuklearmedizin* 1996;35:16.
13. Gallowitsch HJ, Kresnik E, Mikosch P, Lind P. Technetium-99m-sestamibi and ^{99m}Tc-tetrofosmin scintigraphy: alternative scintigraphic methods in follow-up of DTC [Abstract]? *Eur J Nucl Med* 1995;22:909.
14. Nemec J, Nyvltova O, Preiningerova M, et al. Positive thyroid cancer scintigraphy using ^{99m}Tc-tetrofosmin (Myoview): a preliminary report. *Nucl Med Commun* 1995; 16:694–697.
15. Kosuda S, Yokoyama H, Katayama M, et al. Technetium-99m-tetrofosmin and technetium-99m-sestamibi imaging of multiple metastases from differentiated thyroid carcinoma. *Eur J Nucl Med* 1995;22:1218–1220.
16. Klain M, Maurea S, Lastoria S, et al. Technetium-99m-tetrofosmin imaging of differentiated mixed thyroid cancer. *J Nucl Med* 1995;36:2248–2251.
17. Basoglu T, Sahin M, Coskun C, et al. Technetium-99m-tetrofosmin uptake in malignant lung tumors. *Eur J Nucl Med* 1995;22:687–689.
18. Lind P, Gallowitsch HJ, Kogler D, et al. Technetium-99m-tetrofosmin scintimammography: a prospective study in primary breast lesions. *Nuklearmedizin* 1996;35:225–229.
19. Rambaldi PF, Mansi L, Proccacini E, et al. Breast cancer detection with ^{99m}Tc-tetrofosmin. *Clin Nucl Med* 1995;20:703–705.
20. Schlumberger M, Challeton C, De Vathaire F, et al. Radioactive iodine treatment and external radiotherapy for lung and bone metastases from thyroid carcinoma. *J Nucl Med* 1996;37:598–605.
21. Pacini F, Lippi F, Formica N, et al. Therapeutic dose of ^{131}I reveal undiagnosted metastases in thyroid cancer patients with detectable serum thyroglobulin levels. *J Nucl Med* 1987;28:1888–1891.
22. Pineda JD, Lee T, Ain K, et al. Iodine-131 therapy for thyroid cancer patients with elevated thyroglobulin and negative diagnostic scan. *J Clin Endocrinol Metab* 1995;80:1488–14992.
23. Feine U, Lizenmayer R, Hanke JP, et al. Fluorine-18-DG whole-body PET in differentiated thyroid carcinoma. *Nuklearmedizin* 1995;34:127–134.
24. Linden A, Weiβ R, Smolarz K, et al. Bone marrow changes in patients with thyroid carcinoma. *Nucl Med* 1991;30:272–278.

Evaluation of Technetium-99m-MIBI Scintigraphy in Metastatic Differentiated Thyroid Carcinoma

Shinichi Miyamoto, Kanji Kasagi, Takashi Misaki, Mohammad S. Alam and Junji Konishi
Department of Nuclear Medicine, Faculty of Medicine, Kyoto University, Kyoto, Japan

Technetium-99m-methoxyisobutyl isonitrile (^{99m}Tc-MIBI) was evaluated for its ability to detect metastases from thyroid carcinoma. **Methods:** Twenty-seven thyroidectomized patients with metastatic differentiated thyroid carcinoma, of whom 20, 9 and 12 had lung, lymph node and bone metastases, respectively, were examined with ^{99m}Tc-MIBI. The scan results were compared with those of ^{201}Tl and ^{131}I whole-body scans. **Results:** Increased accumulation of ^{99m}Tc-MIBI was observed in lung metastases of 15 patients (75.0%), 12 lymph node metastases (100.0%) and 29 of 31 bone metastases (93.5%). Increased accumulations of ^{201}Tl and ^{131}I scans were seen in, respectively, 16 (80.0%) and 17 (85.0%) of the 20 patients with lung metastases, 12 (100.0%) and 5 (41.7%) of the 12 lymph node metastases and 28 (90.3%) and 27 (87.1%) bone metastases. Because of its better image quality, ^{99m}Tc-MIBI detected more lesions in the lung (n = 38) than ^{201}Tl did (n = 17). **Conclusion:** Technetium-99m-MIBI is clinically useful for detecting metastases from differentiated thyroid carcinoma and deserves clinical application in the postoperative follow-up of such patients.

Key Words: technetium-99m-MIBI; metastatic thyroid cancer; thallium-201; iodine-131

J Nucl Med 1997; 38:352–356

Serum thyroglobulin measurements and whole-body scintigraphy using ^{131}I and ^{201}Tl have been performed to follow postoperative patients with differentiated thyroid carcinoma (*1–5*). Like ^{201}Tl, ^{99m}Tc-MIBI has been reported to localize in various tumors (*6–8*). It also accumulates in thyroid tissues with various pathological conditions, such as Graves' disease (*9*), primary thyroid lymphoma (*10*), thyroid nodules (*11*), Hürthle cell carcinoma (*12*), medullary thyroid cancer (*13*) and distant metastases of thyroid cancer (*14–17*). Our present study evaluated the ability of ^{99m}Tc-MIBI scintigraphy, as compared with ^{201}Tl and ^{131}I scintigraphy, to successfully detect metastases from differentiated thyroid carcinoma.

MATERIALS AND METHODS

Patients

Twenty-seven patients (18 women, 9 men; age 58.2 ± 13.3 yr; range 27–82 yr; mean ± s.d.) with metastatic differentiated thyroid carcinoma who visited Kyoto University Hospital from 1993 to 1995 were studied. All patients had previously undergone a total thyroidectomy. The diagnosis was made on the basis of histological findings observed in the resected specimen. Eighteen and nine patients were diagnosed as having papillary and follicular carcinomas, respectively. All patients were examined for metastatic sites using both ^{99m}Tc-MIBI and ^{201}Tl within an interval of less than 2 wk and then immediately treated with 3.7–5.55 GBq ^{131}I. Thus, most of these patients were hypothyroid at the time of scanning. One week after treatment, whole-body ^{131}I scanning was performed.

A diagnosis of metastases from thyroid carcinoma was based on findings of radiography, CT and MRI, histological findings, increased serum thyroglobulin levels after total thyroidectomy, negative in vitro test results for other tumor markers and absence of nonthyroidal tumors evaluated by radiographic examinations. The diagnosis was confirmed later in those who had a positive ^{131}I scan. Clinical information on all 27 patients is presented in Table 1. Of the 27 patients, 20, 9 and 12 had lung, lymph node and bone metastases, respectively.

Scintigraphy

Ten to 30 min and 3 hr after intravenous administration of 600 MBq ^{99m}Tc-MIBI, whole-body scanning was performed (early and delayed scans, respectively) at 10 cm/min, with both anterior and posterior view images obtained. Spot images of pathological areas were taken if necessary. These images were obtained using a gamma camera and a high-resolution collimator appropriate for low (less than 180 keV) energy. A photopeak of 140 keV with symmetrical 20% window was used.

Whole-body scanning was also performed 10 min after intravenous injection of 74 MBq ^{201}Tl chloride at 10 cm/min. Planar anterior and posterior images were obtained with the same gamma camera and collimator as used for ^{99m}Tc-MIBI scanning. A window at the 80 keV ± 20% was used for photon collection. In some patients, spot images were used to compare ^{99m}Tc-MIBI and ^{201}Tl scans (800-1000 kcts/view versus 400-500 kcts/view, respectively).

When post-therapy ^{131}I scanning was performed, a large field-of-view gamma camera with a high-energy, parallel-hole collimator was used at 10 cm/min. The photopeak was 364 KeV with a symmetrical 20% window.

Received Feb. 26, 1996; revision accepted Jul. 3, 1996.
For correspondence or reprints contact: Shinichi Miyamoto, MD, Dept. of Nuclear Medicine, Faculty of Medicine, Kyoto University, Kyoto 606-01, Japan.

TABLE 1
Clinical Data

Patient No.	Sex	Age	Histology	Metastatic site	^{99m}Tc-MIBI e/d	^{201}Tl	^{131}I	Tg* (μg/liter)
1	M	58	PAC	9th rib	+/+	+	−	1240
2	F	55	FAC	Th4, Th11	+/+	+	+	79.0
3	F	72	PAC	neck LN (1.0 cm) (2 sites)	+/+	+	+	2530
				lung (multiple; <0.2 cm)	−/−	+†	+†	
				1st rib	+/+	+	+	
4	F	69	FAC	lung (multiple; <1.8 cm)	+/n.d.	+†	+	>4000
				femur, pelvis	+/n.d.	+	+	
5	M	68	FAC	1st, 4th and 6th ribs, sternum, sacrum, lumbar spine, sacroiliac joint, pubic bone and femur	+/+	+	+	>4000
6	F	66	PAC	neck LN (2 cm)	+/+	+	−	325
				lung (multiple; 3.0 cm)	+/+	+	−	
7	F	56	PAC	mediastinal LN (2.0 cm)	+/n.d.	+	−	>5000
				lung (multiple; <1 cm)	+/n.d.	+	−	
				skull, scapula, 1st rib	+/n.d.	+	−	
8	F	78	PAC	neck LN (1.5 cm)	+/+	+	−	1690
				mediastinal LN (1.7, 6.5 cm)	+/+	+	−	
9	F	82	FAC	lung (multiple; <0.6 cm)	+/−	+	+	23.7
10	M	27	PAC	lung (multiple; <0.2 cm)	−/−	−	+	123
11	M	57	PAC	mediastinal LN (3.0 cm)	+/+	+	+	323
				lung (multiple; <2.4 cm)	+/−	+	+	
				Th12-L3, iliac bone	+/−	+	+	
12	F	64	PAC	lung (multiple; <0.5 cm)	+/+	+	−	47.5
13	M	47	PAC	lung (multiple; <1.0 cm)	−/−	−	+	>5000
				femur	+/+	+	+	
				sacroiliac joint	+/−	+	+	
14	F	56	PAC	lung (multiple; <2.0 cm)	+/+	+	+	>5000
15	F	66	FAC	lung (multiple; <1.5 cm)	+/−	+	+	318
				Th9	+/−	+	+	
				Th11	+/−	−	+	
16	F	69	FAC	skull, Th (upper portion), sacrum	+/+	+	+	>5000
				L1	−/−	−	+	
17	M	58	FAC	lung (multiple; <0.2 cm)	−/n.d.	+ †	+†	263
18	M	28	PAC	lung (multiple; <0.3 cm)	+/+‡	+	+†	1700
19	F	58	PAC	neck LN (1.2 cm)	+/+	+	+	167
				lung (multiple; <0.7 cm)	+/−	−	+	
				skull	+/−	+	+	
20	F	34	PAC	lung (multiple; <1.0 cm)	+/−‡	+†	+	15.8
21	F	45	PAC	lung (multiple; <0.3 cm)	+/−‡	+†	+†	320
22	F	43	PAC	lung (multiple; <0.1 cm)	+/−‡	+†	+†	198
23	M	63	FAC	lung (multiple; <1.5 cm)	+/−‡	+†	+	1210
24	F	67	PAC	mediastinal LN (0.8 cm)	+/+	+	−	57.5
25	F	61	FAC	lung (multiple; <0.9 cm)	−/−	−	+	1562.3
				9th rib	+/−	+	+	
				femur	−/−	−	+	
26	F	64	PAC	neck LN (1.8 cm)	+/+	+	−	5.1
27	F	61	PAC	mediastinal LN (2.0 cm)	+/+	+	+	>5000
				lung (multiple; <2.0 cm)	+/+	+	+	

*Serum thyroglobulin concentration was determined when suppressive doses of thyroxine were administered.
†Diffuse uptake.
Metastatic thyroid cancer was histogically confirmed in Patients 5 (1st rib), 8 (neck lymph node), 14 (lung) and 26 (neck lymph node). e/d = early scan/delayed scan; PAC = papillary adenocarcinoma; FAC = follicular adenocarcinoma; nd = not done.

Evaluation

Scan images were visually evaluated independently by three nuclear medicine physicians, and consensus was then reached concerning the visualization or nonvisualizaion of lesions. In patients with small diffuse metastatic lesions distributed in the whole lung, the scan was defined as positive when diffuse pulmonary uptake was greater than that in the mediastinum.

Serum Thyroglobulin Measurement

Serum thyroglobulin (Tg) concentrations were determined by immunoradiometric assay using a commercially available kit (normal range, <50 μg/liter). Anti-Tg antibodies that would affect Tg measurements were not detected in any of our patients.

RESULTS

Positive scan results with ^{99m}Tc-MIBI were obtained in 15 (75%) of 20 patients with lung metastases, all 9 patients with lymph node metastases (all 12 lesions) and all 12 patients with bone metastases [29 (93.5%) of 31 lesions]. Early and delayed scans were compared in 13, 8 and 10 patients who showed significantly increased uptake by lung, lymph node and bone metastases, respectively. Technetium-99m-MIBI accumulation

TABLE 2
Comparison of Early and Delayed Technetium-99m-MIBI Scans

Early scan	Delayed scan	Number of patients with: Lung metastases	Lymph node metastases	Bone metastases
+	+	5	8 (11)	6 (17)
+	−	8	0	5 (7)
−	+	0	0	0 (0)
		13	8 (11)	11* (24)

*The total number of patients with bone metastases was 10, because one of them belonged to two groups.

was observed in the early image disappeared at the delayed scan in 8 of 13 patients with lung metastases and 7 of 24 bone metastases (5 of 11 patients), but in none of 11 lymph node metastases (Table 2). Smaller lesions tended to be less clearly visualized on the delayed scan. In Patients 11 and 13, failure to detect metastasis in the pelvic bone on the delayed scan was due to overlapping physiological intestinal radioactivity.

A comparison of ^{99m}Tc-MIBI, ^{201}Tl and ^{131}I scans is presented in Table 3 and Figures 1–3. The incidence of positive scan results with ^{99m}Tc-MIBI, ^{201}Tl and ^{131}I was 75.0% (15/20), 80.0%(16/20) and 85.0% (17/20) for lung metastases (on a patient basis); 100.0% (12/12), 100.0% (12/12) and 41.7% (5/12) for lymph node metastases (on lesion basis); and 93.5% (29/31), 90.3% (28/31) and 87.1% (27/31) for bone metastases (on a lesion basis), respectively. For discordant results, ^{99m}Tc-MIBI was positive and ^{201}Tl negative in one patient (Patient 19) with lung metastases and in one patient (Patient 15) with bone metastases (Table 1). Two patients with lung metastases had positive ^{201}Tl scans but negative ^{99m}Tc-MIBI scans (Patients 3 and 17). Although ^{99m}Tc-MIBI and ^{201}Tl showed similar detectability, the most striking difference was the quality of the images, the former being much better (Figs. 2, 3). Eight patients with lung metastases showed spotty accumulation of ^{99m}Tc-MIBI and ^{201}Tl, with a total of 38 spotty lesions detected by ^{99m}Tc-MIBI and 17 by ^{201}Tl in these patients.

In several patients, a discrepancy between ^{131}I and ^{99m}Tc-MIBI scans was observed (Table 3). Positive ^{131}I and negative ^{99m}Tc-MIBI scans were obtained in three (Patients 10, 13 and 25) with lung metastases and in two (Patients 16, 25) with bone metastases (two lesions). On the other hand, negative ^{131}I and positive ^{99m}Tc-MIBI scans were obtained in three (Patient 6, 7 and 12) with lung metastases, five (Patients 6, 7, 8, 24 and 26) with lymph node metastases (seven lesions) and two (Patients 1, 7) with bone metastases (four lesions).

With regard to detecting metastases during postoperative follow-up, the results were compared on an overall patient basis. Iodine-131 post-therapy scan was positive in 20/27, ^{99m}Tc-MIBI in 25/27, ^{201}Tl in 26/27 and thyroglobulin in 25/27, where the scan result was judged positive when at least one positive scan was seen on a lesion basis, and thyrogloblin was defined as positive when serum levels were higher than 20 μg/liter on suppressive doses of thyroxine.

TABLE 3
Comparison of Technetium-99m-MIBI, Thallium-201 and Iodine-131 Scans in Patients with Lung, Lymph Node and Bone Metastases

Radiotracer	Number of lesions detected: Lung	Lymph node	Bone
^{99m}Tc-MIBI	15/20 (75.0%)	12/12 (100.0%)	29/31 (93.5%)
^{201}Tl	16/20 (80.0%)	12/12 (100.0%)	28/31 (90.3%)
^{131}I	17/20 (85.0%)	5/12 (41.7%)	27/31 (87.1%)

For lung metastases, the calculation was performed on a patient basis.

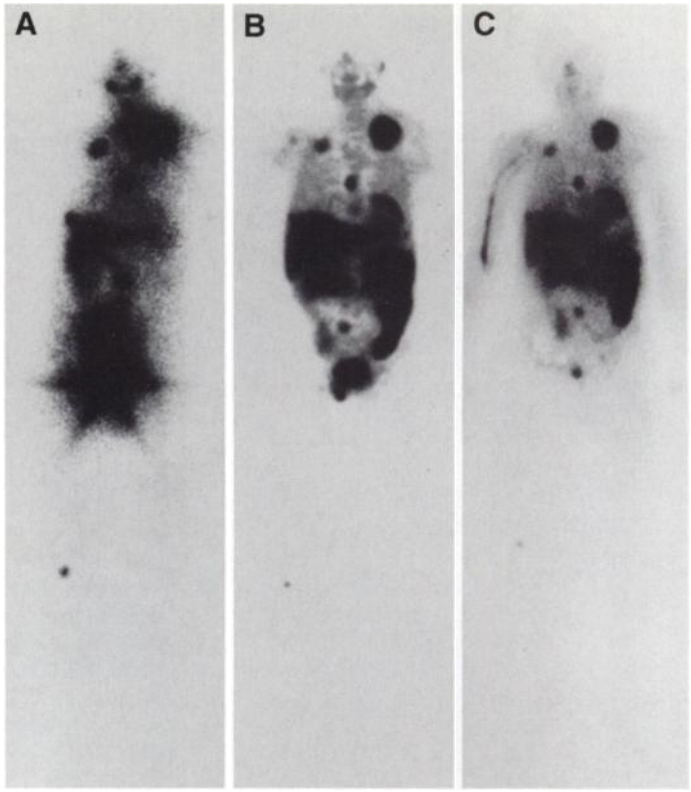

FIGURE 1. (A) Anterior view of Patient 5 after treatment with ^{131}I, (B) ^{99m}Tc-MIBI (early image) and (C) ^{201}Tl scans. Multiple bone metastases are demonstrated in all three images (see Table 1). There is no significant difference in image quality between ^{99m}Tc-MIBI and ^{201}Tl scans.

DISCUSSION

Technetium-99m-MIBI was originally introduced for myocardial perfusion studies (*18*), but its similarities with ^{201}Tl prompted its evaluation in several oncology applications. Thallium mostly follows the potassium pathway through the ATPase-dependent Na^+/K^+ pump, but ^{99m}Tc-MIBI accumulates within cell mitochondria and cytoplasma through electrical potentials generated across membrane bilayers (*19,20*). The cationic charge and lipophilicity of ^{99m}Tc-MIBI, the mitochondrial and plasma membrane potentials of the tumor cells, and cellular mitochondrial content are considered to play a significant role in the mechanism of this agent's tumor uptake (*21*). Recently, much interest was focused on the relationship between ^{99m}Tc-MIBI and the multidrug-resistant P-glycoprotein (*22*), which could not be evaluated in the present study.

Like ^{201}Tl, ^{99m}Tc-MIBI accumulation is not specific for thyroid malignancy. According to Földes et al. (*11*), ^{99m}Tc-MIBI uptake depends mainly on thyroid tissue viability. Although ^{99m}Tc-MIBI and ^{201}Tl may be limited in their ability to differentiate malignant from benign thyroid tumors, their roles in localizing thyroid cancer metastases have been evaluated successfully (*3,5,12,14–17*).

A comparison of early and delayed images revealed that most tumors were more clearly visible on the early scan, and some small-sized lung and bone lesions could not be visualized at the delayed scan. All 12 lymph node metastases were visible on both early and delayed images, possibly because of the rela-

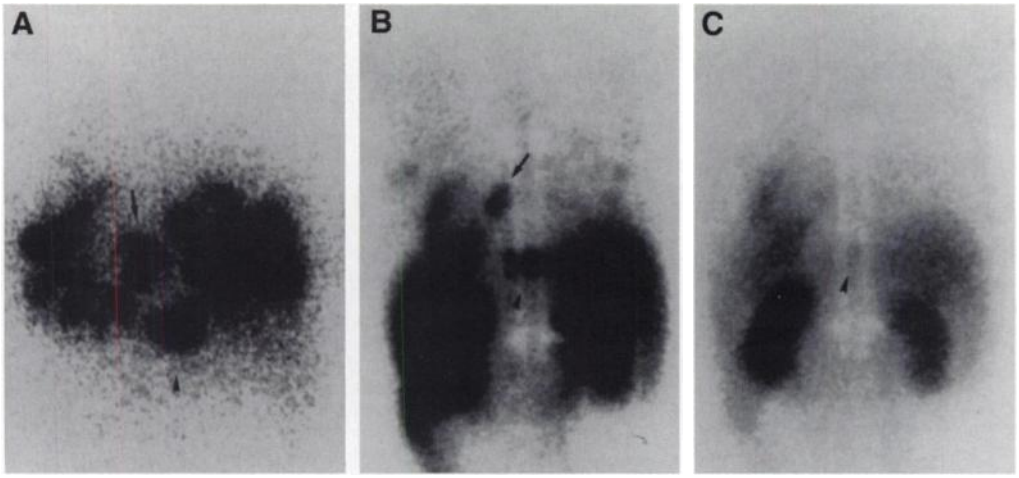

FIGURE 2. (A) Posterior view of ^{131}I, (B) ^{99m}Tc-MIBI and (C) ^{201}Tl scans in Patient 15. Metastatic lesions in the ninth thoracic vertebra (arrow) and the eleventh thoracic vertebra (arrow head) are clearly visualized by ^{131}I and ^{99m}Tc-MIBI, while ^{201}Tl accumulated slightly to the eleventh thoracic vertebra (arrow head) alone. Multiple pulmonary metastases are visualized by both ^{131}I and ^{99m}Tc-MIBI, less clearly and less intensely by the latter, but are hardly recognizable by ^{201}Tl.

tively large size of the tumors or their localization near the surface of the body (6/10 in the neck). In two patients, a metastatic lesion in the pelvic bone was not visualized on the delayed scan because of overlapping physiological intestinal radioactivity. Therefore, we believe that the early scan alone is sufficient to detect metastases, except when they are suspected to be located near the liver, where ^{99m}Tc-MIBI accumulates physiologically on the early scan.

Technetium-99m-MIBI scanning was performed when the patients were hypothyroid. However, Mueller et al. (*17*) reported that MIBI uptake in thyroid carcinoma is independent of TSH stimulation.

In the present study, ^{99m}Tc-MIBI accumulated in lung metastases of 15 patients (75.0%), 12 lymph node metastases (100.0%), and 29 of 31 bone metastases (93.5%). The incidence of ^{201}Tl detection was 80.0% (16/20), 100.0% (12/12) and 90.3% (28/31), respectively. Two patients with multiple small-sized metastases (<0.2 cm in diameter) showed negative ^{99m}Tc-MIBI but positive ^{201}Tl uptake. On the other hand, one patient with lung metastases (<0.7 cm) and one with bone metastases showed positive ^{99m}Tc-MIBI but negative ^{201}Tl uptake. Diffuse pulmonary uptake of ^{201}Tl as well as ^{99m}Tc-MIBI is known to be nonspecific for the disseminated metastases but has been reported to be due to left ventricular dysfunction, smoking and hypertension (*23,24*). We conclude that ^{99m}Tc-MIBI scan is as effective as ^{201}Tl scan in detecting metastases. An additional advantage of ^{99m}Tc-MIBI is the possibility of SPECT, which was not performed in the present study but apparently helps localize lesion. Moreover, although ^{99m}Tc-MIBI and ^{201}Tl had a similar prevalence of positive scans (Table 3), ^{99m}Tc provided better image quality and thus identified more macronodular metastatic lesions in the lung (38 versus 17 lesions).

Similar studies were reported recently (*14–16*). Nemec et al. (*15*) found that ^{99m}Tc-MIBI could detect lung metastases with high sensitivity (35/36). Sundrum et al. (*14*) also reported a high incidence of metastases detection with ^{99m}Tc-MIBI, including local lymph node spread with (47/57). However, these authors did not compare their results with ^{201}Tl images. Dadparvar et al. (*16*), who compared the performance of ^{99m}Tc-MIBI and ^{201}Tl, found that both scans yielded rather low sensitivity (4 of 11 patients for both). They performed delayed imaging 60 min after injection, assuming it increased tumor detectability due to a higher tumor-to-background ratio. However, we could speculate that ^{99m}Tc-MIBI, once accumulated in the tumors of the seven false-negative patients, had cleared by the time of scanning, in view of our finding that the sensitivity of the early scan (10–30 min) is much higher than that of the delayed scan (3 hr) (Table 2). The lower sensitivity, compared with the current and previously reported studies, could also be explained by different patient populations (*14,15*).

As with previous studies (*14,16*), we obtained discordant results between ^{99m}Tc-MIBI and ^{131}I scans in some patients. Negative ^{99m}Tc-MIBI scans and positive ^{131}I scans were obtained in patients with small-sized lung and bone metastases. We assume that the tumors had a high potential for iodine uptake, but in these cases the individual nodule was too small to be detected with ^{99m}Tc-MIBI. On the other hand, ^{99m}Tc-MIBI accumulated more often in lesions (lung metastases from three patients, seven lymph node metastases and four bone metastases in which ^{131}I failed to accumulate, suggesting its applicability in detecting nonfunctioning metastases. Lower detectability of metastases from differentiated thyroid carcinoma by ^{131}I compared to ^{201}Tl was reported by Tonami et al. (*4*) (3/8 versus 7/8) and Hoefnagel et al. (*5*) (26/56 versus 54/56), who used a diagnostic ^{131}I dose. In the present study, even at therapeutic doses, ^{131}I scan was the least sensitive in detecting metastases (20/27 ^{131}I; 25/27 ^{99m}Tc-MIBI; 26/27 ^{201}Tl on a patient basis). Such a discrepancy was clearly shown in cases of lymph node metastases. Higher detectability of lymph node metastases by

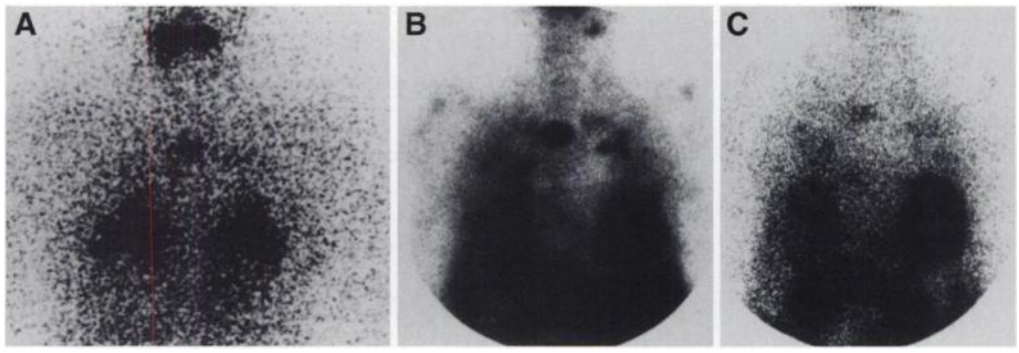

FIGURE 3. (A) Anterior view of ^{131}I, (B) ^{99m}Tc-MIBI and (C) ^{201}Tl scans in Patient 27. Multiple pulmonary metastases are visualized as diffuse pulmonary uptake by ^{131}I, multiple hot spots by ^{99m}Tc-MIBI, and diffuse, faint, uneven uptake by ^{201}Tl. Individual metastatic nodules can hardly be discerned on ^{201}Tl scintigram. Uptake of ^{99m}Tc-MIBI in the metastatic mediastinal lymph node was more intense than that of ^{201}Tl.

^{99m}Tc-MIBI than ^{131}I shown in the present study agress with previous observations by Sundram et al. (*14*) and may also reflect the nonfunctioning nature of the tumors.

CONCLUSION

Although we did not perform a prospective study to evaluate whether ^{99m}Tc-MIBI is useful for early detection of tumor recurrence, the sensitivity of this technique for the detection of metastases warrants its use for clinical follow-up of postoperative patients with thyroid carcinoma. Finally, ^{99m}Tc-MIBI is advantageous over ^{201}Tl, because it detects metastatic lesions.

ACKNOWLEDGMENTS

We thank Miss Yukiko Mieda for administrative assistance and Miss Katsuko Nakagawa and Mr. Toru Fujita for technical assistance.

REFERENCES

1. Van Herle AJ, Uller RP. Elevated serum thyroglobulin: a marker of metastases in differentiated thyroid carcinomas. *J Clin Invest* 1975;56:272–275.
2. Ramanna L, Waxman A, Brachman M, et al. Correlation of thyroglobulin measurements and radioiodine scans in the follow-up of patients with differentiated thyroid cancer. *Cancer* 1985;55:1525–1529.
3. Iida Y, Hidaka A, Hatabu H, Kasagi K, Konishi J. Follow-up study of postoperative patients with thyroid cancer by thallium-201 scintigraphy and serum thyroglobulin measurement. *J Nucl Med* 1991;32:2098–2100.
4. Tonami N, Hisada K. Thallium-201 scintigraphy in postoperative detection of thyroid cancer: a comparative study with ^{131}I. *Radiology* 1980;136:461–464.
5. Hoefnagel CA, Delprat CC, Marcuse HR, de Vijlder JJM. Role of thallium-201 total-body scintigraphy in follow-up of thyroid carcinoma. *J Nucl Med* 1986;27:1854–1857.
6. Hassan IM, Sahweil A, Constantinides C, et al. Uptake and kinetics of ^{99m}Tc-hexakis-2-methoxyisobutylisonitrile in benign and malignant lesions in the lungs. *Clin Nucl Med* 1989;14:333–340.
7. Caner B, Kitapcl M, Unlu M, et al. Technetium-99m-MIBI uptake in benign and malignant bone lesions: a comparative study with technetium-99m-MDP. *J Nucl Med* 1992;33:319–324.
8. Aktolun C, Bayhan H, Kir M. Clinical experience with ^{99m}Tc-MIBI imaging in patients with malignant tumors. Preliminary results and comparison with ^{201}Tl. *Clin Nucl Med* 1992;17:171–176.
9. Kao CH, Wang SJ, Liao SQ, Lin WY, Hsu CY. Quick diagnosis of hyperthyroidism with semiquantitative 30-min ^{99m}Tc-MIBI thyroid uptake. *J Nucl Med* 1993;34:71–74.
10. Scott AM, Kostakoglu L, O'Brien JP, Straus DJ, Abdel-Dayem HM, Larson SM. Comparison of technetium-99m-MIBI and thallium-201-chloride uptake in primary thyroid lymphoma. *J Nucl Med* 1992;33:1396–1398.
11. Földes I, Levay A, Stotz G. Comparative scanning of thyroid nodules with ^{99m}Tc-pertechnetate and ^{99m}Tc-MIBI. *Eur J Nucl Med* 1993;20:330–333.
12. Yen TC, Lin HD, Lee CH, Chang SL, Yeh SH. The role of technetium-99m-sestamibi whole-body scans in diagnosing metastatic Hürthle cell carcinoma of the thyroid gland after total thyroidectomy: a comparison with iodine-131 and thallium-201 whole-body scans. *Eur J Nucl Med* 1994;21:980–983.
13. Lebouthillier G, Morais J, Picard M, Picard D, Chartrand R, D'Amour P. Technetium-99m-sestamibi and other agents in the detection of metastatic medullary carcinoma of the thyroid. *Clin Nucl Med* 1993;18:657–661.
14. Sundram FX, Goh ASW, Ang ES. Role of technetium-99m-sestamibi in localization of thyroid cancer metastases. *Ann Acad Med Singapore* 1993;22:557–559.
15. Nemec J, Nyvltova O, Blazek T, et al. Positive thyroid cancer scintigraphy using technetium-99m-methoxyisobutylisonitrile. *Eur J Nucl Med* 1996;23:69–71.
16. Dadparvar S, Chevres A, Tulchinsky M, Krishna-Badrinath L, Khan AS, Slizofski WJ. Clinical utility of ^{99m}Tc-MIBI imaging in differentiated thyroid carcinoma: comparison with ^{201}Tl and ^{131}I Na scintigraphy and serum thyroglobulin quantitation. *Eur J Nucl Med* 1995;22:1330–1338.
17. Mueller SP, Piotrowski B, Guth-Tougelides B, Reiners C. Technetium-99m-MIBI and ^{201}Tl uptake in thyroid carcinoma [Abstract]. *J Nucl Med* 1988;29(suppl):854.
18. Baillet GY, Mena IG, Kuperus JH, Robertson JM, French WJ. Simultaneous technetium-99m-MIBI angiography and myocardial perfusion imaging. *J Nucl Med* 1989;30:38–44.
19. Strauss H, Pitt B. Thallium-201 as a myocardial imaging agent. *Semin Nucl Med* 1977;7:49–58.
20. Kao CH, Wang SJ, Lin WY, Hsu CY, Liao SQ, Yeh SH. Differentiation of single solid lesions in the lungs by means of SPECT with ^{99m}Tc-MIBI. *Eur J Nucl Med* 1993;20:249–254.
21. Chiu ML, Kronauge JF, Piwnica WD. Effect of mitochondrial and plasma membrane potentials on accumulation of hexakis (2-methoxyisobutylisonitrile) technetium(I) in cultured mouse fibroblasts. *J Nucl Med* 1990;31:1646–1653.
22. Rao V, Chiu M, Kronauge J, Piwnica-Worms D. Expression of recombinant human multidrug resistance P-Glycoprotein in insect cells confers decreased accumulation of ^{99m}Tc-sestamibi. *J Nucl Med* 1994;35:510–515.
23. Datz FL. Diffuse pulmonary uptake. In: *Gamuts in nuclear medicine*, 3rd ed. St. Louis, MO: Mosby Year Book Inc; 1995;382–383.
24. Miller DD, Heyl BL, Walsh RA. Lung uptake of technetium-99m hexamibi isonitrile during acute reversible ischemic left ventricular dysfunction in conscious dogs. *Circulation* 1988;78:(suppl):II-387.

Tumor Quantitation and Monitoring in Whole-Body Planar Technetium-99m-Sestamibi Imaging

Serge D. Van Kriekinge, Guido Germano, Charles Forscher, Gerald Rosen, Pawan Gupta and Alan D. Waxman

Department of Medical Physics and Imaging and Division of Nuclear Medicine, Department of Imaging, The Burns and Allen Research Institute, Cedars-Sinai Medical Center; The Cedars-Sinai Comprehensive Cancer Center; Department of Radiological Sciences, UCLA School of Medicine; Los Angeles, California

We have developed a completely automatic software package to normalize, rigidly register and elastically match serial whole-body planar images from patients with limb tumors. Variations in tumor uptake and size are analyzed and quantitated by the software. **Methods:** The software consists of a chain of modules incorporating several automatic algorithms. A rigid registration algorithm aligns images by translation and rotation based on feature points corresponding to the patient's neck and bladder. An elastic matching algorithm generates a grid for each image in a sequence by combining thresholding and local feature analysis in the head, torso and leg regions. A linear warping algorithm then interpolates pixel values and locations to make the grid points in all images coincide with the grid points of one of them (the reference image). All images in a sequence are normalized based on brain uptake. Quantitation of tumor uptake and size is performed in all images using an ROI automatically determined from a single user-selected seed point. **Results:** The software was tested on four 2-image and one 3-image sequences from five patients (11 images). Quantitative measurements of body contour overlap show an average intrasequence agreement of 73.4%, 78.7% and 91.5% for unregistered, rigidly registered and rigidly registered + matched images, respectively. **Conclusion:** Our method represents an objective, quantitative tool to measure tumor activity in sequential whole-body scintigraphic images, and may help assess tumor response to chemotherapy or radiation therapy.

Key Words: tumor quantitation; whole-body image registration; planar scintigraphy image registration

J Nucl Med 1997; 38:356–361

The comparison of whole-body planar scintigraphic images recorded sequentially in conjunction with chemotherapy or radiation therapy is an important tool in assessing the effectiveness of a treatment. Technetium-99m-sestamibi and ^{201}Tl have been used frequently to detect and evaluate primary and metastatic tumors (*1–8*). Changes in the tumor size or uptake between serial images are currently assessed subjectively

Received March 25, 1996; revision accepted July 1, 1996.

For correspondence or reprints contact: Guido Germano, PhD, Director, Nuclear Medicine Physics, Cedars-Sinai Medical Center A047 N, 8700 Beverly Blvd., Los Angeles, CA 90048.